Vol. 42, No. 3 (2020) 513-527, DOI: 10.24874/ti.854.02.20.08

Tribology in Industry

www.tribology.rs

RESEARCH

Enhancing the Mechanical and Reciprocating Wear Behavior of Functionally Graded A359 Aluminium Alloy Through Heat Treatment

N. Radhika[a]*, R. Jojith[a], N.S. Hari Thiagarajan[a], M. Ruthraprakash[a]

[a] *Department of Mechanical Engineering, Amrita School of Engineering, Coimbatore Amrita Vishwa Vidyapeetham, India -641 112.*

Keywords:

A359 Aluminium
Functionally graded material
Heat-treatment
Reciprocating wear
Delamination wear

* Corresponding author:

N. Radhika
E-mail: n_radhika1@cb.amrita.edu

Received: 29 February 2020
Revised: 22 May 2020
Accepted: 28 August 2020

A B S T R A C T

This paper discusses on improving the mechanical and tribological characteristics of homogeneous and functionally graded A359 aluminium alloy processed through gravity and centrifugal casting respectively, through T6 heat treatment. Microstructural observation confirmed uniform and gradient structure for homogeneous and functionally graded casts respectively. Maximum micro-hardness values were observed at 10 hours aging time followed by a significant drop due to over aging. After T6 treatment, 38 and 40 % improvement in micro-hardness, 11 and 13.4 % improvement in tensile strength was observed on comparing as-cast homogeneous and functionally graded material respectively. Wear evaluation was performed for all the regions of as-cast and heat treated functionally graded material and homogeneous casts by varying load (15-35 N) and sliding distance (500-1500 m). Maximum wear resistance was observed for heat treated functionally graded material (outer) under the effect of sliding distance. Wear analysis revealed predominant delamination wear mechanism on worn surfaces.

1. INTRODUCTION

The affordability and processability in the manufacturing sector is provided a clear and credible pathway by the introduction of Functionally Graded Materials (FGM). The design of alloy components are improved by integrating and processing the concept of FGMs, hence producing commercial materials with tailored properties [1]. Centrifugal casting, a simple pressure casting method is selected among different FGM processing methods, in which the force of gravity is employed through the spinning of mould, to form cylindrical bulk FGM components having dense and fine grained structure [2,3]. Due to the influence of centrifugal action upon the molten metal, minimal cast defects are observed in FGMs, when compared to gravity casts [4]. They possess a position dependent microstructure, chemical composition or atomic order, which results in the continuous variation of mechanical, electrical and thermal properties of material along radial direction [5]. Functionally

graded Aluminium–Silicon (Al-Si) alloys have become the key materials for processing automotive and aerospace components owing to their significant good resistance to wear and high strength to weight ratio, which leads to a considerable fuel economy improvement [6]. EN AC 48000, an extensively used piston alloy, exhibited poor ductility and elongation during failure, which eventually led to fatigue and catastrophic failure in the piston skirt. This can be avoided by employing FGM component having enhanced ductility in the skirt along with improved mechanical and thermal resistance at the piston crown [7]. Dasam Kim et al fabricated FGM using AA6063 aluminum-based alloy having superior strength and hardness to protect the material from external shock while the excellent ductility property provided improved flexibility to the material, thus enhancing the workability [8]. Bhansali et al confirmed that increasing material hardness leads to increase in resistance to wear under high load conditions [9]. Due to the poor ductility property of Al-Si alloy components having high strength, these components undergo T6 thermal treatment, solution treatment for required hours, followed by quenching in hot water and then age hardening above recrystallization temperature [10]. Eutectic silicon spheroidises during solutionising, thus accounting for the improved ductility in T6 tempered condition. Both aging time and temperature are said to have a significant influence on the final properties, as the break-up of eutectic silicon is defined by the plates' thermal degradation initiated at crystal defects [11,12].

At severe load conditions, heat treated FGMs exhibit the best combination of tribo-mechanical properties. The wear behavior of Al-Si alloy depends mostly on process parameters such as load, frequency, sliding distance, mechanical properties, composition and interfacial conditions [13,14]. Gomes et al and Rajeev et al confirms that under optimum conditions, Al-Si alloys frictional force and wear rate increases with increase in load [15,16] whereas under the influence of higher sliding speeds, a non-linear decrease in wear properties are observed [17,18]. As steel is the widely used material and aluminium is the successor, the aluminium-steel tribo-pair is preferred for studying wear [19]. Liu et al. concludes that the alloy wear is mainly caused by several wear mechanisms such as melt lubrication wear, oxidation wear, delamination wear, and seizure. At lower sliding speeds and loads, oxidation wear mechanism is the dominant wear mechanism whereas at higher loads, metal-metal interface leads to severe wear at higher temperatures, higher than recrystallization temperature [20].

Based on the literature, it is observed that very limited work has been explored in Al - 9Si (A359) aluminium alloy. Hence, the present study focusses on the enhancement of mechanical and tribological properties of homogeneous and FGM cast components through T6 heat treatment. The components are fabricated using liquid metallurgy techniques A comparative analysis was also performed to understand how the heat treatment improved the properties. Microstructural, mechanical and wear behavior of the cast components (homogeneous and FGM) were analyzed under as-cast and heat treated conditions (T6 tempered). Wear behavior was analyzed using cylindrical pins on a linear reciprocating tribometer. Worn surface analysis of heat treated FGM and homogeneous casts were performed using Scanning Electron Microscopy (SEM).

2. SELECTION OF MATERIAL AND EXPERIMENTAL PROCEDURES

This section describes the selection of material, processing route and the procedure followed for microstructural characterization, hardness, tensile and reciprocating wear studies.

2.1 Material selection

Al-Si alloys are widely used for tribological studies from which A359 alloy is chosen owing to its ductility, low co-efficient of thermal expansion, high strength at elevated temperatures and resistance to wear under heat treated conditions. These alloys are used for manufacturing automotive part applications such as cylinder liners, piston rings and brake drums. Elemental composition of the cast functionally graded aluminium alloy (A359) was tested using Optical Emission Spectroscopy (OES) and the obtained results are tabulated in Table 1.

Table 1. Elemental composition (at %) for A359 Aluminium alloy.

Elemental Composition (at %)	As per standard	Cast Ingot
Si	8.5 – 9.5	9.045
Fe	0.2 – 0.4	0.325
Mn	< 0.4	0.318
Mg	0.2 – 0.6	0.417
Ti	< 0.2	0.106
Cu	< 0.2	< 0.2
Al	Balance	Balance

2.2 Processing Technique

FGM and homogenous A359 aluminium alloy cast components are synthesized by centrifugal and liquid metal gravity casting techniques respectively. The alloy cut pieces are melted in a graphite crucible by heating to 760 °C, employing an electric resistance furnace (Fig. 1a). Using a mechanical stirrer rotating at 250 rpm, a vortex is maintained inside the crucible. This is done in an argon gas atmosphere, to avoid chemical reactions. In order to achieve a pronounced cast, permanent metallic moulds are used in both fabrication techniques, which facilitates directional solidification under controlled cooling rates. Simultaneously, metallic dies are pre-heated to 300 °C to avoid casting defects (shrinkage, cold shut and misrun) during solidification. Employing a hopper channel arrangement, the molten melt is easily transferred to a rotating centrifugal die (1000 rpm) (Fig. 1b), where the centrifugal force generated by the rotating die and gravitational force acts on the molten metal until solidification. For liquid gravity casting technique, molten metal is directly transferred to the pre-heated metallic die. After natural cooling, FGM and homogeneous cast components are obtained in hollow and solid cylindrical shapes with dimensions $Ø_{(outer)}$100 x $Ø_{(inner)}$60 x 100 mm and Ø20 x 150 mm respectively. The density study was carried out by taking three cut specimens from multiple locations. The tests were performed based on Archimedes' principle. The average density was experimentally concluded as 2.72 g/cc.

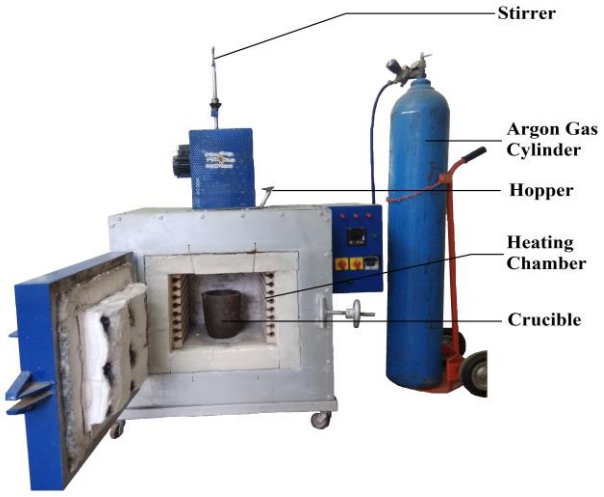

(a)

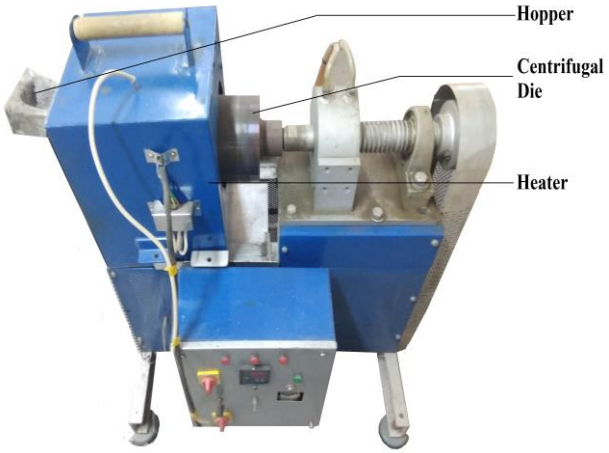

(b)

Fig. 1. (a) Electric Resistance Furnace, (b) Centrifugal cast setup.

2.3 Heat treatment

For comparative study, all cast components under heat treatment under T6 temper conditions to enhance the material properties. Soaking time and temperatures for the treatment are chosen as per the recommendations mentioned in the ASM handbook (Volume 2) [21]. Heat treatment process involves following steps.

- Initially, the samples are heated to 540 °C from room temperature for 10 hours' duration. This treatment in achieving a homogeneous concentration in the solid solution and aids in dissolving any trace elements formed during solidification.
- To attain super-saturated solid solution, the specimens are quenched to room temperature in hot water (50 – 75 °C).

- Artificial aging of samples to permit precipitation from the super-saturated condition, followed by cooling in air to room temperature - 155 °Cfor an aging period of 6 to 12 hours.

2.4 Microstructural characterization

Metallographic evaluation on the test specimens are performed on Zeiss Axiovert CA Inverted optical metallurgical microscope. For 20 mm thick FGM component, three layers are considered for metallographic characterization, layers at 2 mm depth from the outer and inner peripheries are considered as outer and inner layers respectively, and 10 mm from the outer periphery is considered as the middle layer. Due to rapid cooling at the molten metal-metallic die interface, skin formation takes place at the outer periphery, and minor casting defects at the inner periphery. Hence, characterization is carried out at 2 mm away from both peripheries. Metallographic characterization is carried at the cross-section of the homogeneous cast component. Wear samples (worn surfaces and debris collected during experimentation) are evaluated and analyzed using a ZEISS Field Emission Gun Scanning Electron Microscope (FEG-SEM) equipped with EDS micro-analyzer through X-rays.

2.5 Micro hardness testing

Micro hardness testing is performed on MITUTOYO INDENTEC Vickers hardness tester, based on the recommended guidelines as per ASTM E384 standard. For FGM alloy, hardness behavior is evaluated at a 2 mm distance from outer and inner peripheries respectively (outer and inner layers) and at a distance of 10 mm from the outer periphery (middle layer). A load of 500 gf is applied to mark a diamond indentation on the specimen for a dwell time of 15 seconds. Five specimens are considered for each layer and for each specimen, the test is repeated at five different locations.

2.6 Tensile testing

A359 alloy as-cast and heat treated (FGM and homogeneous) samples are tested using TINIUS OLSEN Universal Tensile Testing Machine. Testing is performed as per ASTM B557 standard. For evaluating the FGM tensile strength, three testing zones are considered based on the diverse cooling rates and microstructural changes from outer to inner periphery, 1-10 mm, 11 - 20 mm and 5 – 15 mm from outer periphery as chosen as outer zone, inner zone and middle zone respectively.

2.7 Reciprocating wear testing

Using a pin on flat tribometer setup (DUCOM) (Fig. 2), linear reciprocating wear tests are performed on samples prepared based on the recommendations mentioned in ASTM G133 standard [15,22].

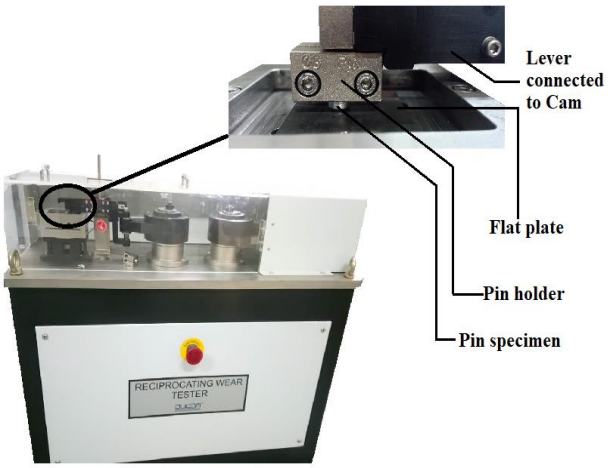

Fig. 2. Reciprocating Pin and Plate Setup.

The experimental parameters are also defined as per the standards. A cylindrical specimen of height 15 mm and Ø9.57 mm behaves as the contact pin whereas EN 31 steel flat plate is chosen as the counter plate. FGM pins are prepared from three individual zones of the ring. The experiments are performed under room temperature by varying load (15, 25 and 35 N) and sliding distance (500, 1000 and 1500 m). Wear rate is measured by using the formula, Specific Wear rate = Wear volume / Normal load per sliding distance. Any change in the specimen weight before and after each experiment is measured using a weigh balance of least count 0.001 mg. The coefficient of friction is calculated by the load cells and data is recorded using WINDUCOM software.

3. RESULTS AND DISCUSSIONS

The following sections explain the comparative analysis and results of as-cast and heat treated FGM and homogeneous casts.

3.1 Metallography study

Figures 3a - 3d shows the as-cast A359 optical micrographs for FGM and homogeneous components in which large portion of aluminium grains and alpha-eutectic silicon as grain boundaries are observed. In general, the eutectic silicon will not uniformly distribute, but tends to be connected at inter-dendritic boundaries. In as-cast FGM, uneven cooling conditions are observed from outer to inner periphery due to the thermal mismatch developed between the molten metal and pre-heated metallic die. It is observed that the eutectic silicon did not undergo uniform distribution and most of silicon accumulated at the grain boundaries [23]. A gradual grain refinement is observed from inner towards outer periphery, wherein fine grains are observed in the outer region (Fig. 3a) and marginally coarser grains are observed on moving towards inner region in radial direction (Figs. 3b and 3c) [24]. Trace amount of titanium in the heat/melt acts as grain refining agents during solidification. In homogeneous casts (Fig. 3d) grain structure remains almost similar to inner region of the FGM 50 μm.

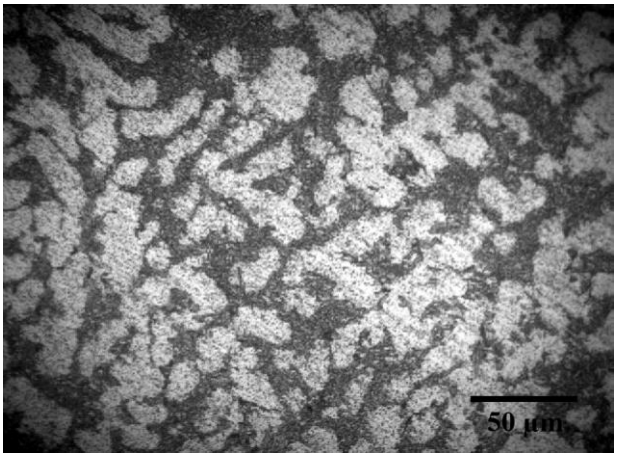

(a)

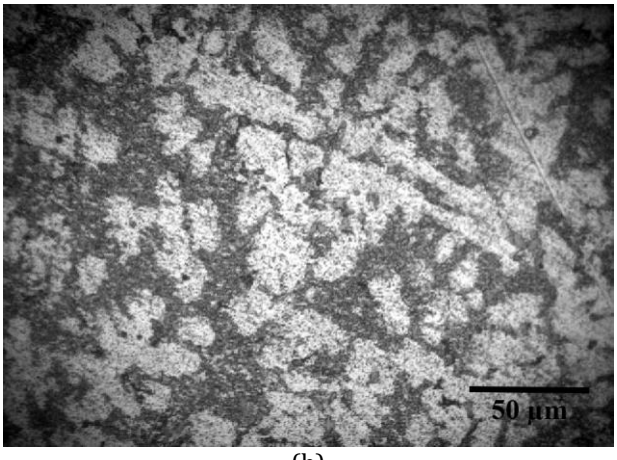

(b)

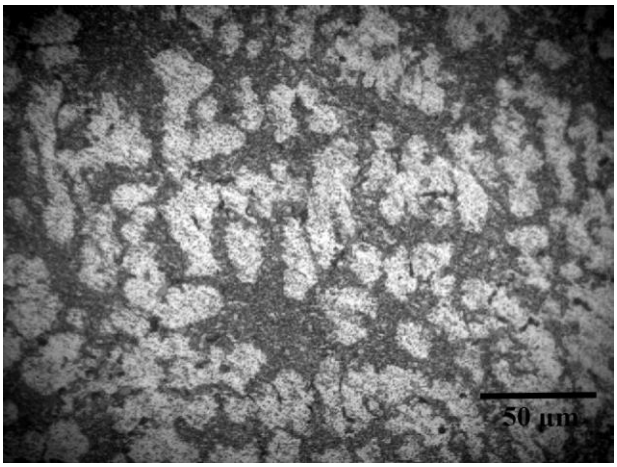

(c)

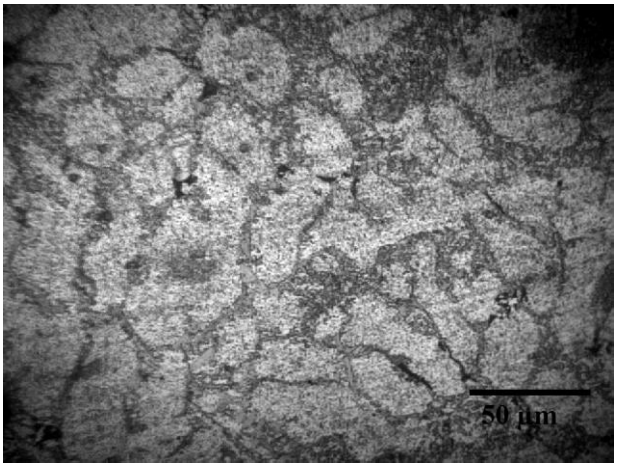

(d)

Fig. 3. Microstructures of as-cast alloy (a) FGM Outer region (b) FGM Middle region, (c) FGM Inner region (d) Homogeneous cast.

Figures 4a - 4d depicts the microstructures of heat treated FGM and homogeneous A359 aluminium alloys. At solidus temperature, the alloy displays good solid solubility and it decreases with temperature under equilibrium conditions. Eutectic Si morphology has a crucial part in minimizing the alloying elements segregation. In the beginning of solutionising, the Si platelets in the unmodified structure breaks down into fine fragments of spheroidised Si, which then gradually undergoes spheroidisation during artificial aging [25]. Prolonged solution treatment leads to coarsening effect, so samples are solution treated for 10 hours. As the aging temperature reaches 10 hours, meager Mg_2Si (precipitate) phase formation occurs and the coarse spheroidised eutectic Si becomes gradually fine. Beyond 10 hours, spheroidised eutectic Si becomes coarser due to over aging phenomenon [26]. In as-cast FGM casts, there is a significant

microstructural change observed along the radial direction whereas in heat treated condition, due to the formation of single phase solid solution in solutionising stage, a trivial change in microstructure is observed (Figs. 4a - 4c). Similar transformation is observed for homogeneous casts (Fig. 4d) [27].

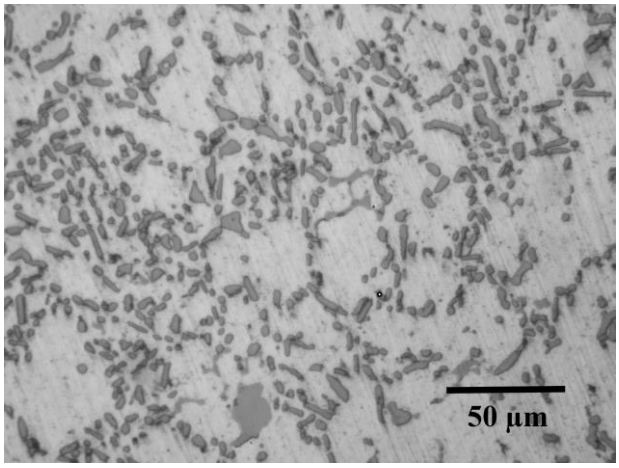

(a)

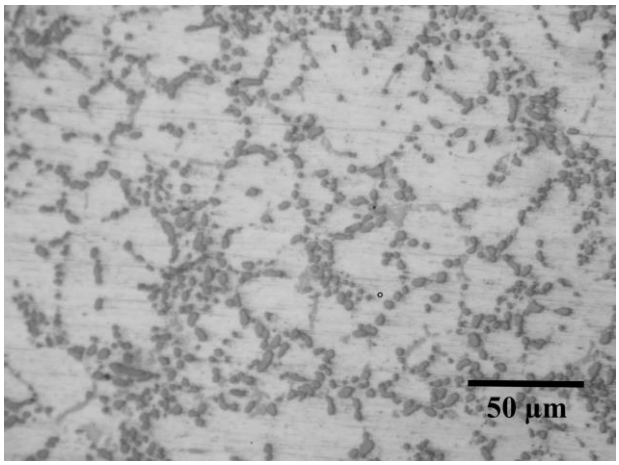

(b)

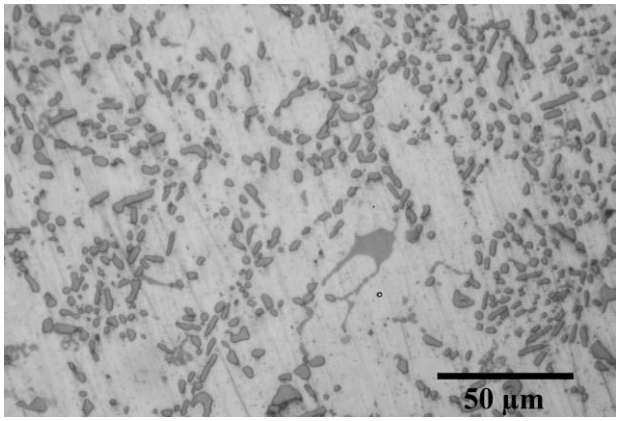

(c)

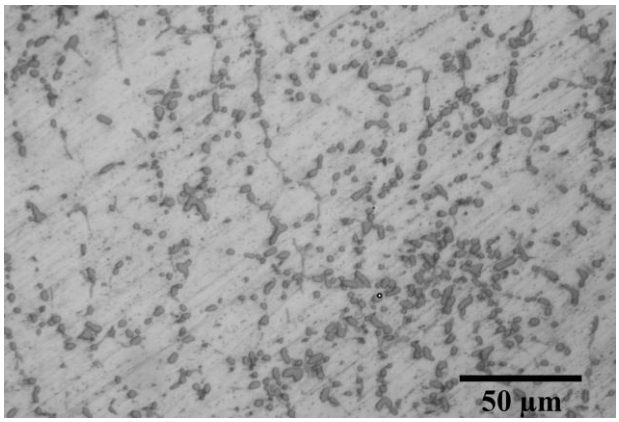

(d)

Fig. 4. Microstructures of heat treated alloy (a) FGM Outer region, (b) FGM Middle region, (c) FGM Inner region, (d) Homogeneous cast.

XRD analysis of heat treated A359 FGM alloy (Fig. 5) confirms the presence of various elements through the XRD peaks at 2θ = 28.4713° for silicon and 2θ = 38.5080° for aluminium. Meager phase formation takes place due to the presence of trace amount of elementals like Mg and Cu.

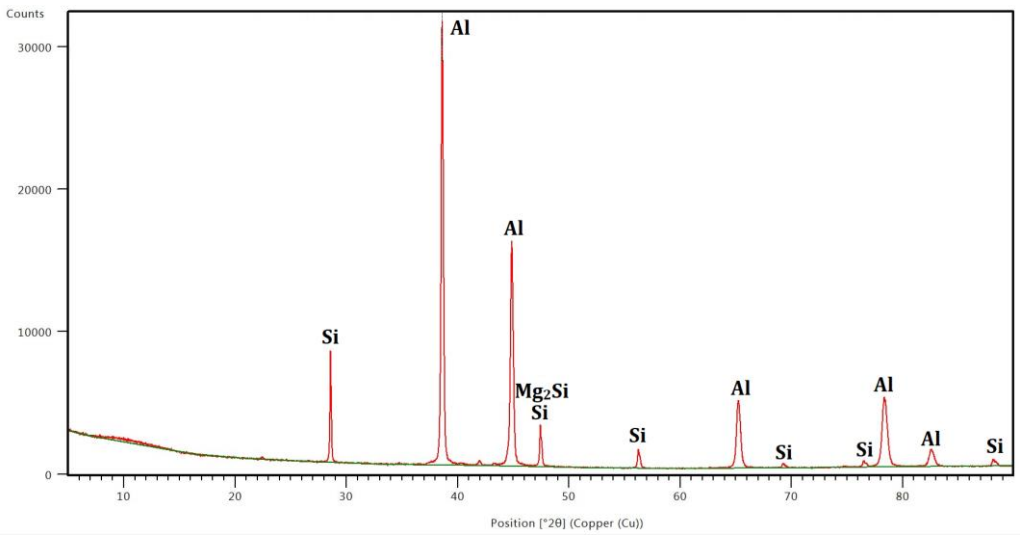

Fig. 5. XRD patterns for heat treated A359 FGM Alloy.

3.2 Hardness study

Figure 6 illustrates the hardness variations of the as-cast and heat treated A359 FGM and homogeneous alloy. FGM and homogeneous alloy display an average hardness of 105.1 HV and 85.2 HV respectively in as-cast condition and increases to 144.53 HV and 123.4 HV respectively under heat treatment. At the A359 alloy outer regions, the as-cast and heat treated hardness values are 110.7 HV and 146.4 HV respectively and then the hardness values decrease for both on moving towards middle and inner regions. It is concluded that heat treated FGM (outer) and homogenous alloy showed nearly 38 and 45 % improvement in micro-hardness values over as-cast FGM and homogenous alloy respectively. This confirms that heat treatment has a significant improvement in the material properties.

In as-cast alloy, hardness values decrease from outer region to inner region along the radial direction due to the controlled cooling conditions at the outer periphery and the uneven cooling conditions at the inner periphery [3]. The microstructure of outer layer of FGM (Fig. 3a) observed supports the inference made, as the molten metal is in direct contact with the preheated metallic die. This increases the rate of solidification, which influences the formation of fine grains in the outer layers. At inner regions, low hardness values are observed due to slow cooling rate, which forms coarser grains (Fig. 3c). In homogeneous casts, poor cooling rates are observed along with the presence of minor defects like porosities and blow holes (Fig. 3d), which reduces the hardness values observed. In heat treated condition, the FGM and homogeneous alloy hardness increases linearly during artificial aging with respect to time till 10 hours, followed by a significant drop in hardness values after 10 hours, owing to the coarsening effect of spheroidised eutectic silicon (Figs. 4a - 4d), which decreases the surface energy [10]. This phenomenon is technically termed as over aging. It is concluded from the comparative analysis of micro-hardness values with existing literature that heat treated FGM alloy had better hardness values than heat treated FGM A356 alloy and T6 treated Aluminium 6061 alloy [28,29].

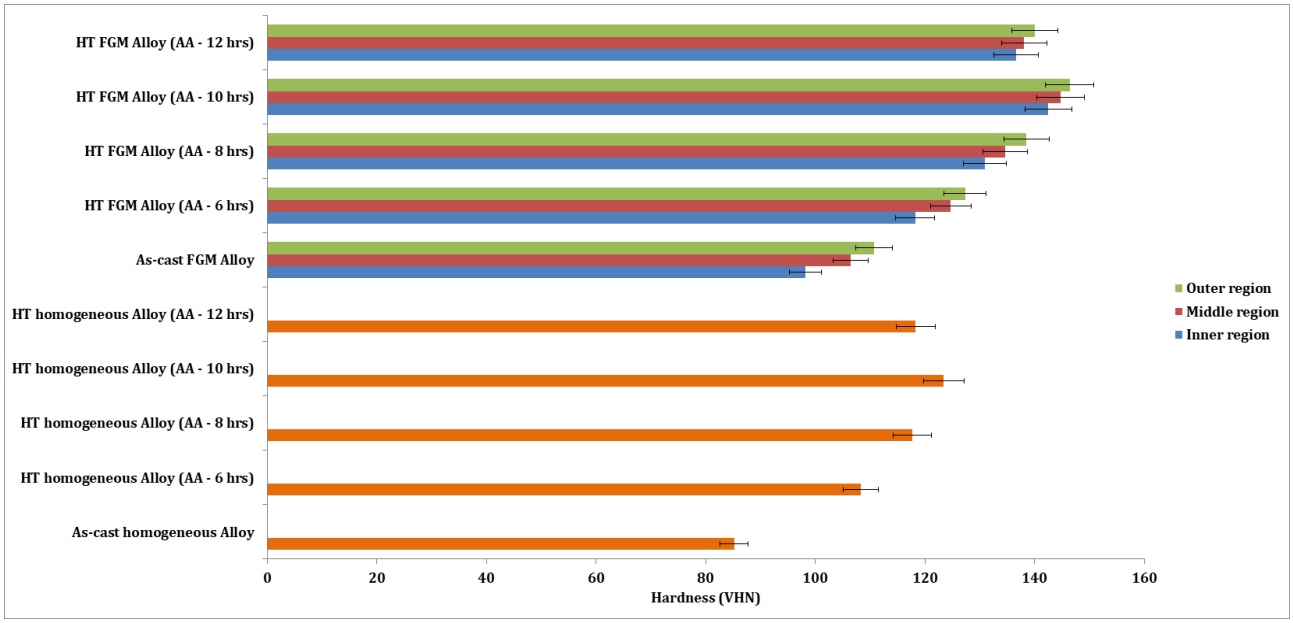

Fig. 6. Micro hardness for as-cast and heat treated FGM and homogeneous alloys.

3.3 Tensile study

Figure 7 depicts the tensile strength plot of as-cast and heat-treated samples. It is evident that the FGM and homogeneous components has an average tensile strength of 173.6 MPa and 165.3 MPa respectively in as-cast condition and 187.06 MPa and 179.3 MPa respectively in heat treated condition. For the outer zone of as-cast and heat treated A359 alloy, the tensile strength values are 178.8 MPa and 189.4 MPa respectively and then the strength reduces on moving towards middle and inner regions for both conditions. In as-cast condition, tensile strength marginally varies from outer region to inner region due to formation of marginal fine grain structure under controlled cooling conditions, as observed from Figs. 3a – 3c. In heat treated condition (Figs. 4a - 4c), the thermally induced dislocations in the aluminium alloy (formed upon quenching) serves as heterogeneous nucleation sites during age hardening process for the formation of eutectic silicon in spheroidised form [27]. This improves the tensile strength and ductility with respect to corresponding as-cast tensile strength of various samples. It is concluded that heat-treated FGM (outer) and homogenous alloy showed nearly 7.75 and 8.5 % improvement in tensile strength over as-cast FGM and homogenous alloy respectively, which confirmed the role of heat treatment.

Proper analysis of the fracture often yields much information on the contributing factors and helps to identify the type of fracture. Fractography analysis is performed on the fractured surfaces of heat treated FGM (outer) and homogeneous cast alloys, (Figs. 8a and 8b) to know the fracture morphology of tensile samples.

SEM observations on heat treated FGM (outer) shows various fracture surface topographies in Fig. 8a. In the fractured surface, micro-crack initiation and early crack growth is observed. The surfaces are dull and shiny with some evidence of plastic deformation. Cleavage type of fracture is evident with large participates of voids under the action of axial load along with partial plastic deformation. Combination of cleavage and partial plastic deformation changes the stress pattern during the propagation of fracture in the orientation of grains [30]. This indicates a mixed mode (ductile – brittle failure) fracture on heat treated FGM sample.

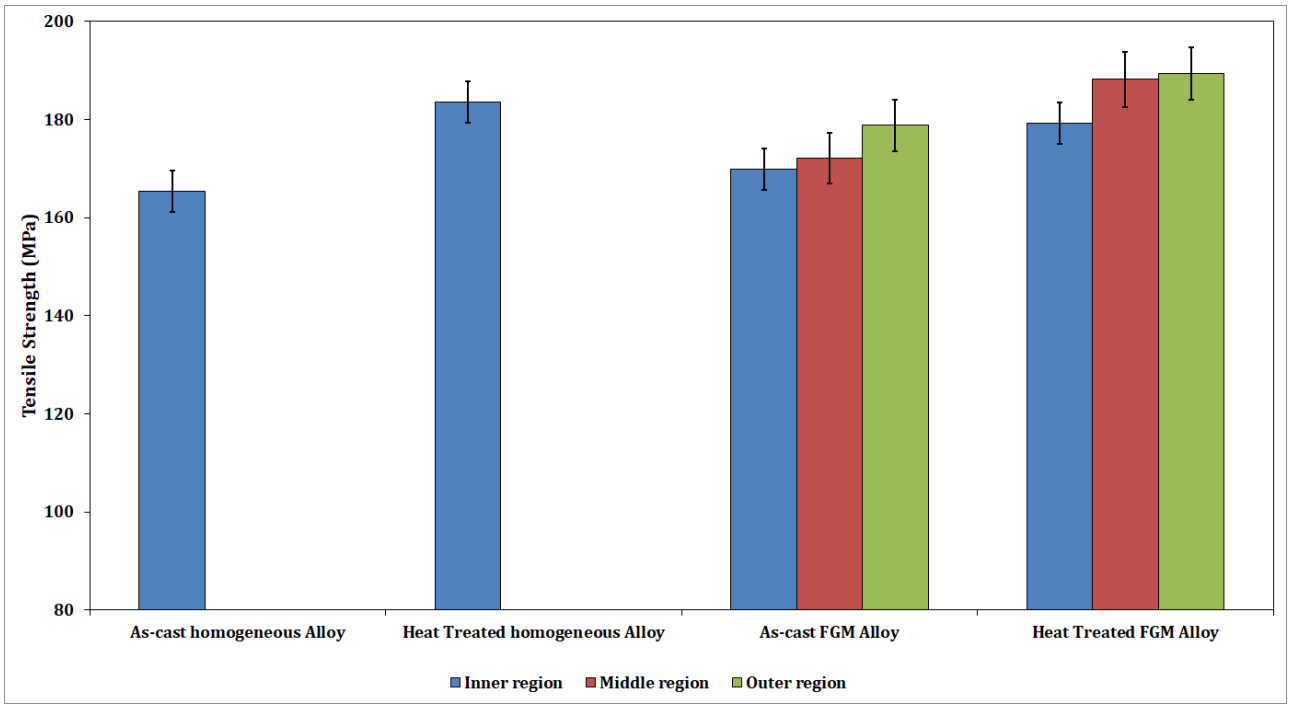

Fig. 7. Tensile strength values of as-cast and heat treated FGM and homogeneous alloy.

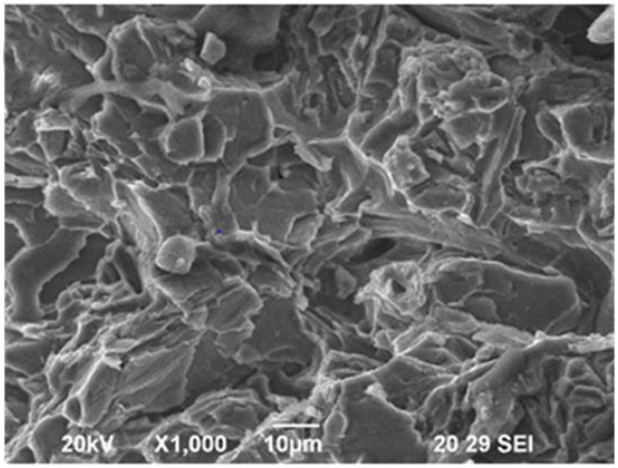

(a)

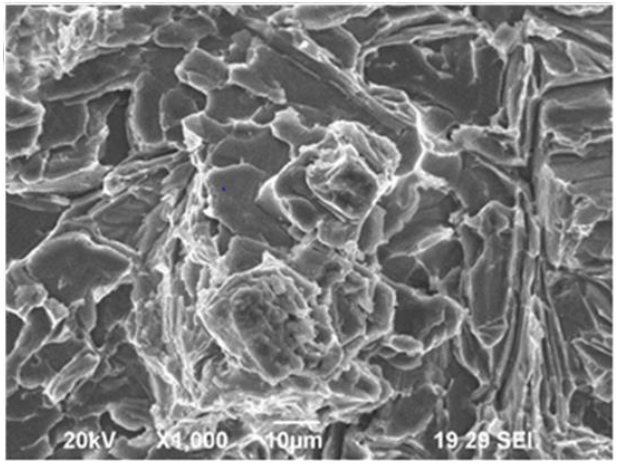

(b)

Fig. 8. Fracture SEM image (a) heat treated FGM alloy (outer) (b) heat treated homogeneous alloy.

In Fig. 8b, comparatively shinier cleavages are observed with the evidence of partial plastic deformation at the edges. This also indicates a mixed mode failure (ductile – brittle failure) with poor or little ductility on heat treated homogeneous alloy. Comparing the heat treated A359 FGM alloy tensile strength values with existing literature, it was confirmed that the FGM alloy displayed near close tensile strength values to heat treated A356 FGM alloy and friction stir processed Aluminium 6061-T6 alloy [28,31].

3.4 Wear study

Following paragraphs discusses how applied load and sliding distance influences the wear rate and co-efficient of friction under low and extreme conditions. The specimens are analyzed using SEM to further understand the wear mechanisms.

At 15 N load and 1000 m sliding distance, as-cast and heat treated FGM (outer) shows a wear rate of 0.00023 mm^3/Nm and 0.000165 mm^3/Nm respectively (Fig. 9), which confirms a 28.2 % decrease in wear rate and conclude that heat treated FGM (outer) exhibits superior wear resistance when compared to as-cast FGM (outer).

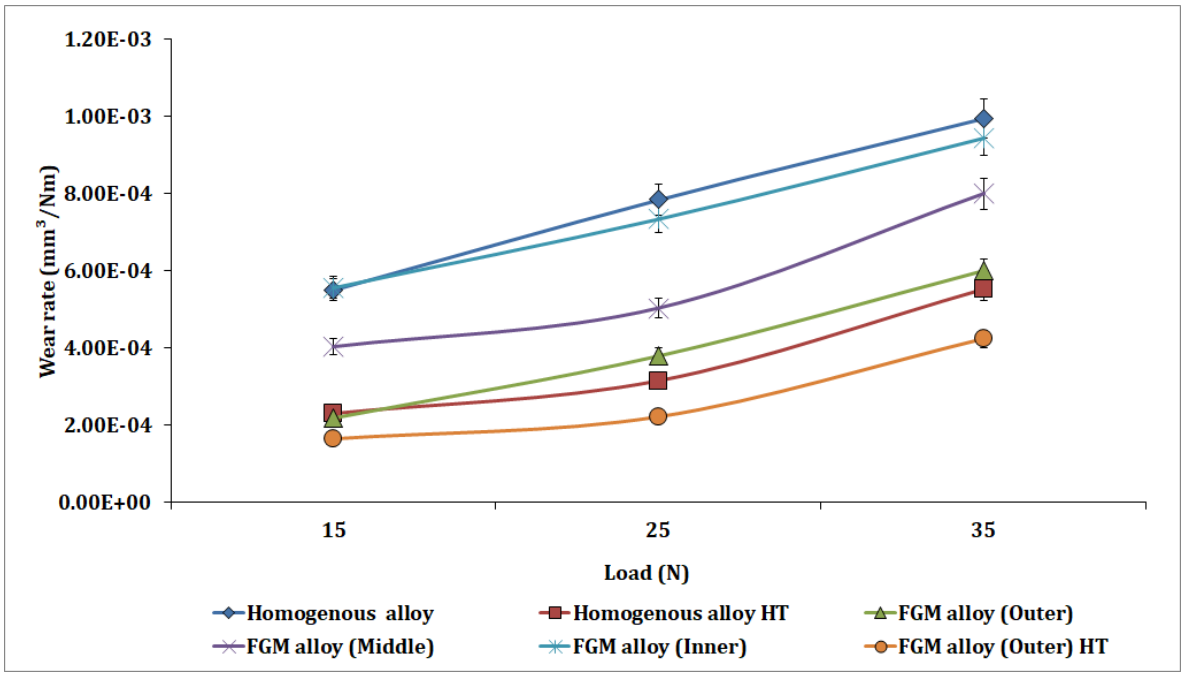

Fig. 9. Effect of wear rate under varying load.

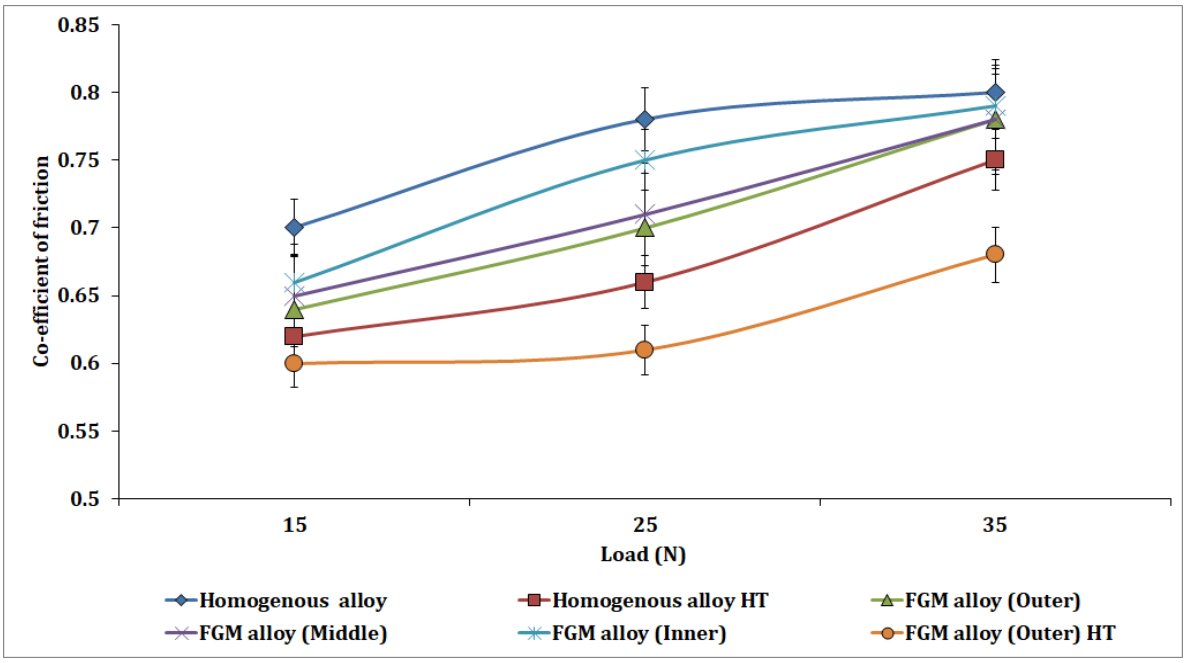

Fig. 10. Effect of co-efficient of friction under varying load.

Similar trend was observed in other two regions of FGM casts in all other load conditions. Homogeneous alloy exhibits marginally poor resistance to wear, when compared with FGM casts. Co-efficient of friction increases with increase in load linearly for all the cast components under study (Fig. 10). This is attributed to the spheroidised eutectic silicon formation in heat treated condition and the sound casts produced under the sway of centrifugal action with a smaller number of casting defects [15]. This increases the hardenability of the heat treated samples, which simultaneously decreases the material removal rate. From 15 to 35 N for both as-cast and heat treated samples, it is concluded that with increase in load, the weight loss rate increases, owing to the abrasion rate increase which leads to material detachment as wear debris and leads to more weight loss in the specimen [11,32]. It is concluded that heat treated FGM outer layer and homogenous alloy displayed superior wear resistance than as-cast FGM outer layer and homogenous alloy at high load applications. Comparative analysis confirmed a wear rate decrease of nearly 30 and 46 % in heat treated homogenous alloy and FGM outer layer, which confirmed that heat treatment improved the wear resistance of the alloy.

Figures 11a and 11b shows the wear morphology of heat treated FGM alloy (outer) at 15 and 35 N loads with constant 1000 m sliding distance respectively.

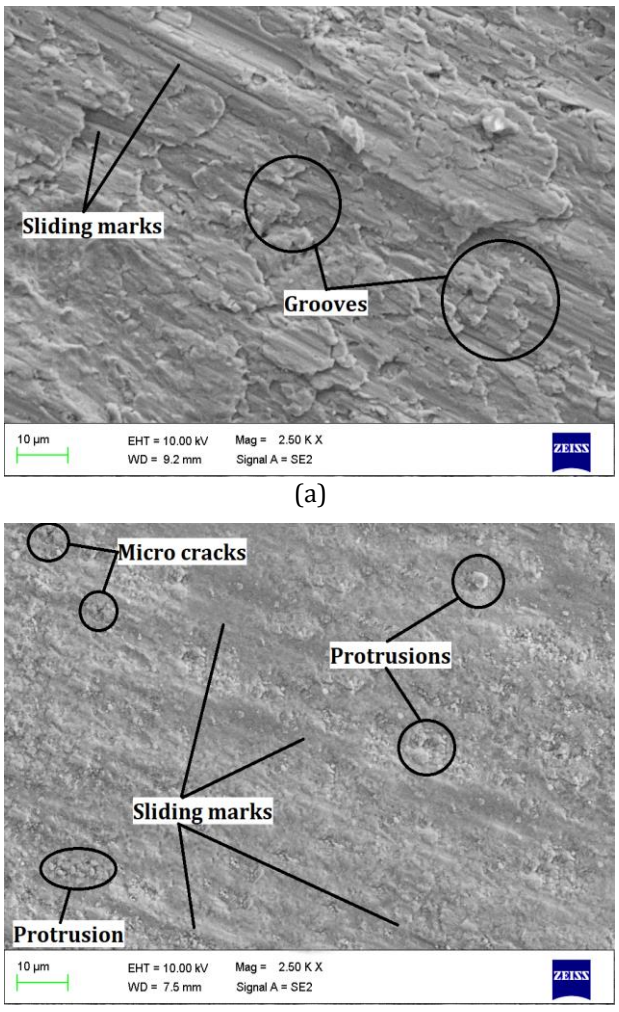

Fig. 11. Wear morphology of heat treated FGM alloy (outer) (a) 15 N load, (b) 35 N load.

Figure 11a shows parallel sliding marks and grooves along the sliding directions upon the worn surface. Aluminium alloy as a light alloy, has low yield stress values under dry reciprocating condition. Its shear force on the sliding surface brings about plastic deformation in the grain area [33], but formation of spheroidised eutectic Si after heat treatment increases the resistance to deformation. Less surface damage is observed, when compared to other conditions. Protrusions, micro cracks and grooves on the worn surface reveal severe surface damage in the sliding direction (Fig. 11b). Work hardening increases the crack sensitivity and therefore, the stress imposed during the wear test propagates these cracks [34]. Transfer of Al from test specimen to the steel counter face by adhesion is observed in the form of plate like ribbon structures which characterizes the morphology of wear debris. Severe wear regime upon the pins is due to the influence of temperature and plastic deformation at the higher loads [35].

Figures 12 and 13 shows the effect of sliding distance on the reciprocating wear rate and co-efficient of friction under a constant load (25 N) respectively. For all wear samples under study, it is confirmed that wear rate significantly increases with increase in sliding distance (Fig. 12). As sliding distance increases, heat treated FGM alloy (outer) shows good resistance to wear, with a minimum wear rate of 0.0005685 mm^3/Nm. Figure 13 confirms that co-efficient of friction increases with increase in sliding distance for all the cast components. Material removal rate increases due to low frequency and higher strokes, which increases the material softening [36].

At 500 m sliding distance, a decrease in wear rate is brought about by the dominant strain hardening effect. Based on the geometrical features of wear scar, wear rate of the heat treated components significantly dropped for lesser sliding distances. As the sliding distance increases from 500 to 1500 m, tribological interactions tend to take place with the influence of self-mated conditions, which increases the adhesion component of friction and thus wear rate increases [34,37]. At a sliding distance of 500 m, the obtained sliding speed is comparatively low, so the energy generated by friction is not sufficient to raise the temperature at the interface [13]. As-cast and heat treated worn surfaces of the homogeneous and FGM components lacks hardenability at longer sliding distance values, which indicates high level of surface damage.

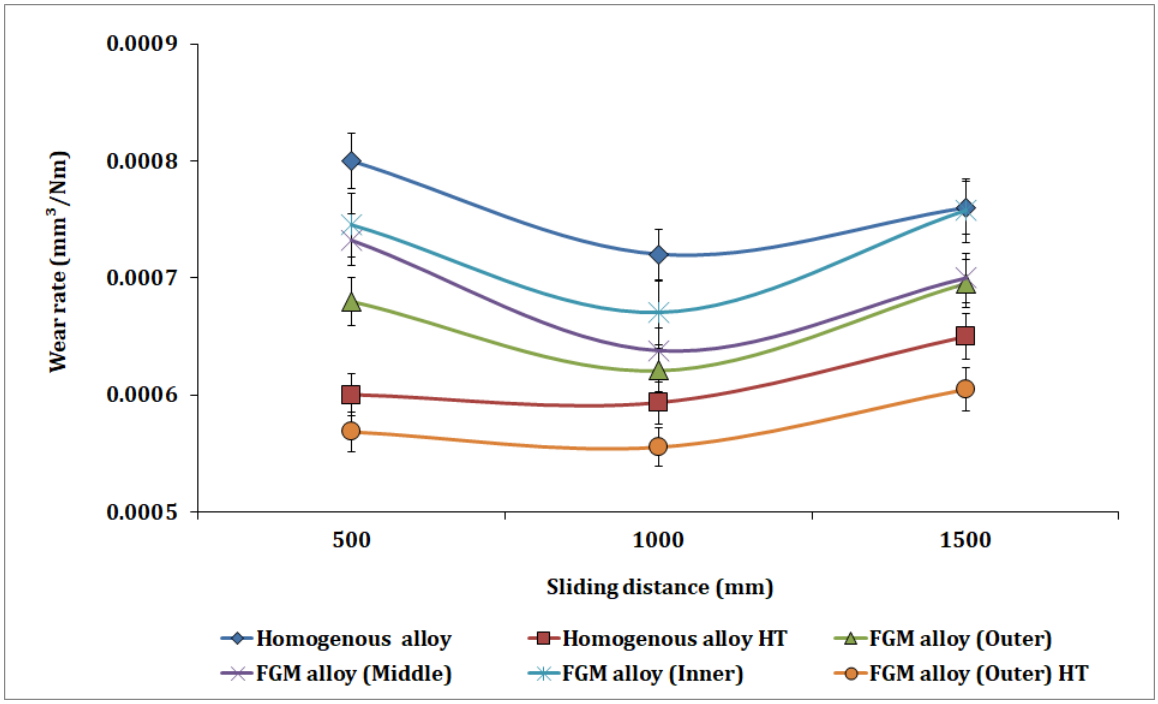

Fig. 12. Effect of wear rate under various sliding distances

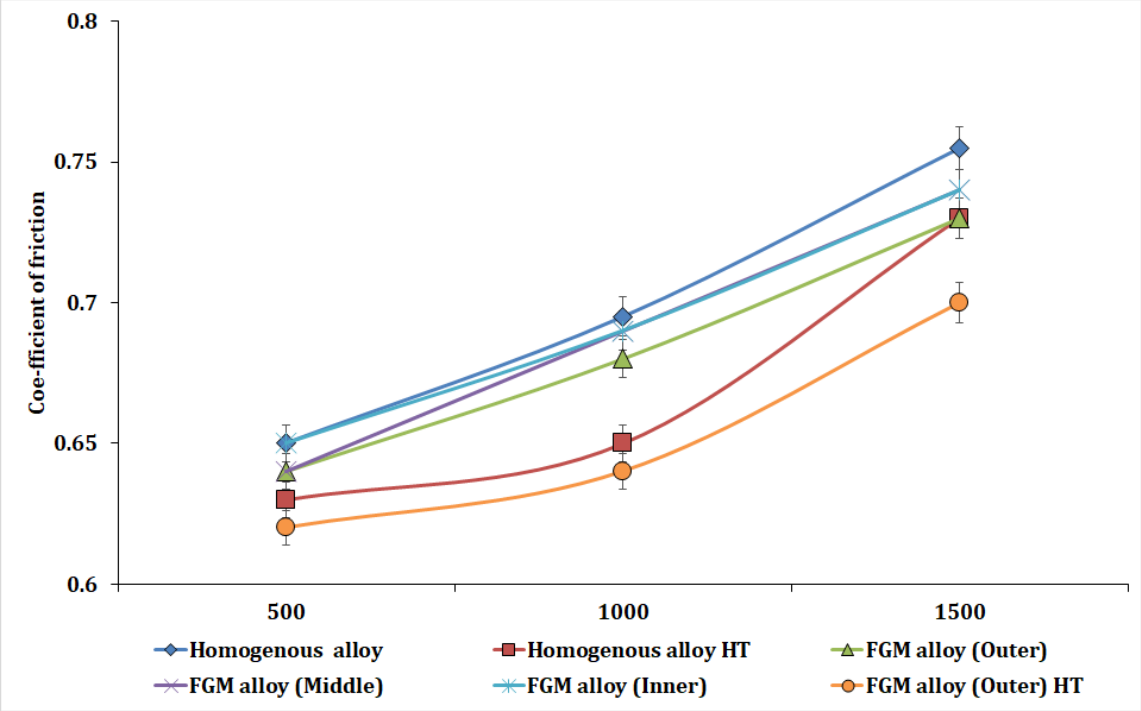

Fig. 13. Effect of co-efficient of friction under various sliding distances.

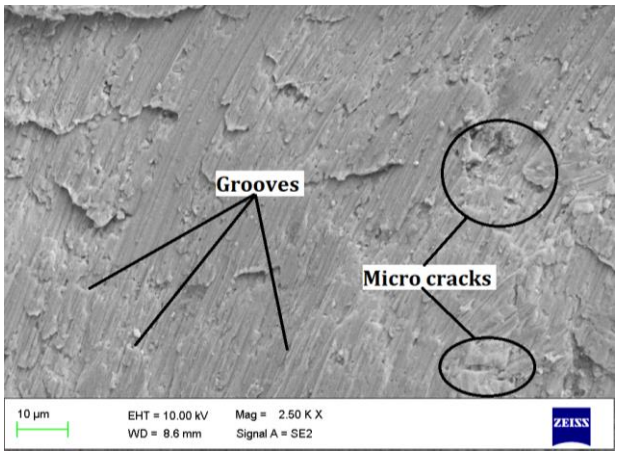

(a)

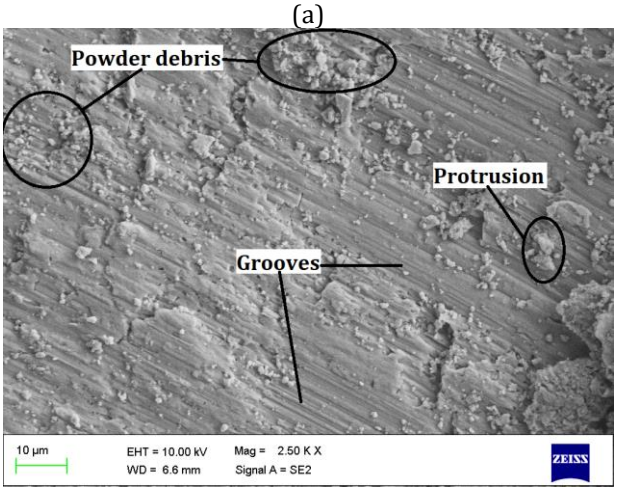

(b)

Fig. 14. Wear morphology of heat treated FGM alloy (outer) at (a) 500 m sliding distance, (b) 1500 m sliding distance.

Worn surface analysis is performed only for heat treated FGM outer layer, as it shows good resistance to wear, when compared to all other samples. Worn surface analysis of the specimen at 500 m sliding distance (Fig. 14a) depicts minimal wear tracks alongside micro cracks and grooves, which concludes less surface damage. At 1500 m sliding distance, worn surface morphology reveals severe surface damage for the pin, with small material patches being sheared off in the direction opposite to sliding alongside micro cracks, grooves along with protrusions, un-compacted powdery debris of Al on the worn surface (Fig. 14b). Due to the plastic deformation, the abrasive particle causes extra ploughings which causes severe surface damage, thus resulting in heavy delamination [38]. Comparing the linear reciprocating wear rates observed for heat treated FGM A359 alloy with existing literature, it was observed that heat treated functionally graded A359 alloy displayed superior wear resistance than heat treated functionally graded A356 alloy [28].

Figure 15a depicts the wear debris SEM morphology, wherein large sized particles are observed as loose wear debris due to plastic fracture. Due to delamination wear, the flake-type debris generated along with ferritic oxides increases the wear rate. Energy Dispersive Spectroscopy (EDS) analysis (Fig. 15b) confirms

the presence of oxygen and iron on the surface which affirms the formation of various elemental oxides along with 'Fe'. These oxides form a tribo-layer called 'Mechanically Mixed Layer' on the surface of heat treated FGM (outer) sample, due to which a marginal.

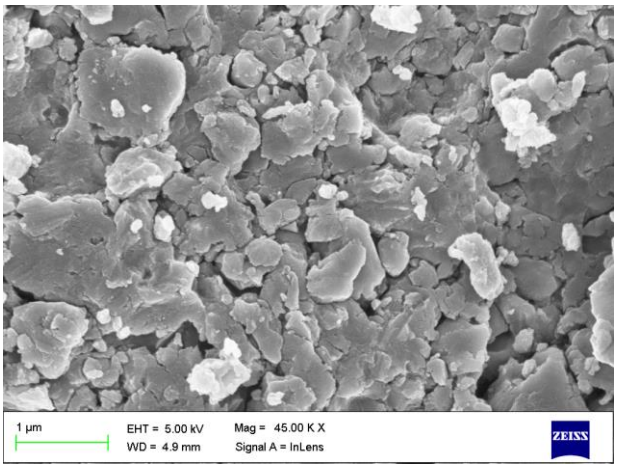

(a)

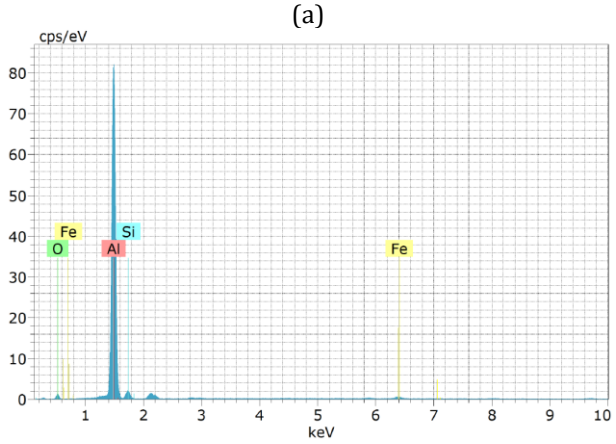

(b)

Fig. 15. (a) Wear debris SEM, (b) EDS of wear debris.

Hence, from the experimental studies conducted, it can be concluded that the heat treatment performed following ASM standards had a significant influence on the material properties. An improvement of nearly 38 to 45% was observed for micro-hardness, nearly 7.8 to 8.5% improvement in tensile strength and an improvement in wear resistance of 30 to 46% was observed when comparing as cast alloys (homogeneous and FGM) to heat treated alloys.

4. CONCLUSION

A359 aluminium alloy was successfully processed by using gravity casting and horizontal centrifugal casting. Specimen cut from casts were heat treated following T6 thermal conditions. Following conclusions were drawn based on the experiments conducted.

- FGMs exhibited a gradient distribution of properties along the radial direction from outer to inner periphery. Metallographic observation for as-cast and heat treated FGM alloy displayed a formation of finer to coarse grains, towards inner periphery along radial direction, whereas homogeneous cast alloys have uniform grain structure. Thermally treated FGM component exhibited superior properties due to eutectic silicon spheroidisation.

- Hardness tests performed on as-cast and heat treated conditions of A359 FGM alloy concluded superior surface hardness at outer layers when compared to A359 homogeneous alloy.

- Tensile tests concluded that A359 FGM alloy (outer zone) exhibited superior tensile strength and showed 13% improvement over as-cast FGM (outer) and 10% improvement over heat treated A359 homogeneous alloy. Fractography shows mixed mode (ductile-brittle) failure for both the casts under comparison.

- Wear rate and co-efficient of friction increased with increasing applied load and sliding distance. Heat treated FGM alloy showed improved wear resistance than as-cast alloy.

- Worn morphology analysis revealed protrusions, voids, micro-cracks and flaky type wear debris on the worn surface of the heat treated FGM samples, which indicated delamination wear mechanism.

5. FUTURE SCOPE

A359 (Al-9Si) as alloy or in metal matrix composite is of large interest to automobile and aerospace industry sectors wherein, their attractive mechanical and tribological properties can be made use in wide range of applications. It also can be used as a potential material in high temperature applications, wherein the enhanced material properties under thermal treatment can be employed.

Acknowledgement

We are so thankful to AR&DB Organization for providing the financial support. [ARDB/01/2031877/M/1]

REFERENCES

[1] I.M. El-Galy, M.H. Ahmed, B.I. Bassiouny, *Characterization of functionally graded Al-SiCp metal matrix composites manufactured by centrifugal casting*, Alexandria Engineering Journal, vol. 56, iss. 4, pp. 371-381, 2017, doi: 10.1016/j.aej.2017.03.009

[2] T.P.D. Rajan, B.C. Pai, *Developments in processing of functionally gradient metals and metal–ceramic composites: a review*, Acta Metallurgica Sinica (English Letters), vol. 27, pp. 825-838, 2014, doi: 10.1007/s40195-014-0142-3

[3] E. Jayakumar, A.P. Praveen, T.P.D. Rajan, B.C. Pai, *Studies on tribological characteristics of centrifugally cast SiCp-reinforced functionally graded A319 aluminium matrix composites*, Transactions of the Indian Institute of Metals, vol. 71, pp. 2741-2748, 2018, doi: 10.1007/s12666-018-1442-5

[4] N. Radhika, *Comparison of the mechanical and wear behaviour of aluminium alloy with homogeneous and functionally graded silicon nitride composites*, Science and Engineering of Composite Materials, vol. 25, iss. 2, pp. 261-271, 2018, doi: 10.1515/secm-2015-0160

[5] E. Fracchia, S. Lombardo, M. Rosso, *Case Study of a Functionally Graded Aluminum Part*, Applied Sciences, vol. 8, iss. 7, p. 1113, 2018, doi: 10.3390/app8071113

[6] N. Radhika, R. Raghu, *Development of functionally graded aluminium composites using centrifugal casting and influence of reinforcements on mechanical and wear properties*, Transactions of Nonferrous Metals Society of China, vol. 26, iss. 4, pp. 905-916, 2016, doi: 10.1016/S1003-6326(16)64185-7

[7] M.B. Karamış, A.A. Cerit, B. Selçuk, F. Nair, *The effects of different ceramics size and volume fraction on wear behavior of Al matrix composites (for automobile cam material)*, Wear, vol. 289, pp. 73-81, 2012, doi: 10.1016/j.wear.2012.04.012

[8] D. Kim, K. Park, M. Chang, S. Joo, S. Hong, S. Cho, H. Kwon, *Fabrication of functionally graded materials using aluminum alloys via hot extrusion*, Metals, vol. 9, iss. 2, p. 210, 2019, doi: 10.3390/met9020210

[9] K.J. Bhansali, R. Mehrabian, *Abrasive wear of aluminum-matrix composites*, JOM, vol. 34, pp. 30-34, 1982, doi: 10.1007/BF03338093

[10] D.P. Myriounis, S.T. Hasan, T.E. Matikas, *Microdeformation behaviour of Al–SiC metal matrix composites*, Composite Interfaces, vol. 15, iss. 5, pp. 495-514, 2008, doi: 10.1163/156855408784655292

[11] D. Apelian, S. Shivkumar, G.A.F.S. Sigworth, *Fundamental aspects of heat treatment of cast Al-Si-Mg alloys*, AFS transactions, vol. 97, pp. 727-742, 1989.

[12] V. Paramo, R. Colás, E. Velasco, S. Valtierra, *Spheroidization of the Al-Si eutectic in a cast aluminum alloy*, Journal of Materials Engineering and Performance, vol. 9, pp. 616-622, 2000, doi: 10.1361/105994900770345467

[13] Md.A. Islam, Z. Farhat, *Wear of A380M aluminum alloy under reciprocating load*, Journal of Materials Engineering and Performance, vol. 19, pp. 1208-1213, 2010, doi: 10.1007/s11665-010-9595-3

[14] L.V. Priyanka Muddamsetty, N. Radhika, *Effect of Heat Treatment on the Wear Behaviour of Functionally Graded LM13/B_4C Composite*, Tribology in Industry, vol. 38, no. 1, 2016.

[15] J.R. Gomes, A. Ramalho, M.C. Gaspar, S.F. Carvalho, *Reciprocating wear tests of Al–Si/SiCp composites: A study of the effect of stroke length*, Wear, vol. 259, iss. 1-6, pp. 545-552, 2005, doi: 10.1016/j.wear.2005.02.088

[16] V.R. Rajeev, D.K. Dwivedi, S.C. Jain, *Effect of load and reciprocating velocity on the transition from mild to severe wear behavior of Al–Si–SiCp composites in reciprocating conditions*, Materials & Design, vol. 31, iss. 10, pp. 4951-4959, 2010, doi: 10.1016/j.matdes.2010.05.010

[17] C. Subramanian, *Effects of sliding speed on the unlubricated wear behaviour of Al-12.3 wt.% Si alloy*, Wear, vol. 151, iss. 1, pp. 97-110, 1991, doi: 10.1016/0043-1648(91)90349-Y

[18] R. Jojith, N. Radhika, *Fabrication of LM 25/WC functionally graded composite for automotive applications and investigation of its mechanical and wear properties*, Journal of the Brazilian Society of Mechanical Sciences and Engineering, vol. 40, p. 292, 2018, doi: 10.1007/s40430-018-1217-2

[19] D. Kumar, H. Roy, B.K. Show, *Tribological behavior of an aluminum matrix composite with Al4SiC4 reinforcement under dry sliding condition*, Tribology Transactions, vol. 58, iss. 3, pp. 518-526, 2015, doi: 10.1080/10402004.2014.990594

[20] Y. Liu, R. Asthana, P. Rohatgi, *A map for wear mechanisms in aluminium alloys*, Journal of materials science, vol. 26, pp. 99-102, 1991, doi: 10.1007/BF00576038

[21] J.R. Davis, ASM *handbook*, ASM International, vol. 2, 1990.

[22] J.M. Gómez de Salazar, M.I. Barrena, *Influence of heat treatments on the wear behaviour of an AA6092/SiC25p composite*, Wear vol. 256, iss. 3-4, pp. 286–293, 2004, doi: 10.1016/S0043-1648(03)00389-2

[23] C.M. Cepeda-Jiménez, J.M. García-Infanta, A.P. Zhilyaev, O.A. Ruano, F. Carreño, *Influence of the supersaturated silicon solid solution concentration on the effectiveness of severe plastic deformation processing in Al–7 wt.% Si casting alloy*, Materials Science and Engineering: A, vol. 528, iss. 27, pp. 7938-794, 2011, doi: 10.1016/j.msea.2011.07.016

[24] T.P.D. Rajan, E. Jayakumar, B.C. Pai, *Developments in solidification processing of functionally graded aluminium alloys and composites by centrifugal casting technique*, Transactions of the Indian Institute of Metals, vol. 65, pp. 531-537, 2012, doi: 10.1007/s12666-012-0191-0

[25] C.L. Xu, Y.F. Yang, H.Y. Wang, Q.C. Jiang, *Effects of modification and heat-treatment on the abrasive wear behavior of hypereutectic Al–Si alloys*, Journal of Materials Science, vol. 42, pp. 6331-6338, 2007, doi: 10.1007/s10853-006-1189-y

[26] H.R. Lashgari, A.R. Sufizadeh, M. Emamy, *The effect of strontium on the microstructure and wear properties of A356–10% B_4C cast composites*, Materials & Design, vol. 31, iss. 4, pp. 2187-2195, 2010, doi: 10.1016/j.matdes.2009.10.049

[27] E. Sjölander, S. Seifeddine, *The heat treatment of Al–Si–Cu–Mg casting alloys*, Journal of Materials Processing Technology, vol. 210, iss. 10, pp. 1249-1259, 2010, doi: 10.1016/j.jmatprotec.2010.03.020

[28] R. Jojith, N. Radhika, *Heat-treatment studies on mechanical and reciprocating wear behaviour of functionally graded A356 alloy,* Materials Research Express, vol. 6, iss. 11, p. 1165c2, 2019, doi: 10.1088/2053-1591/ab4dd7

[29] C.F. Tan, S.M. Radzai, *Effect of hardness test on precipitation hardening aluminium alloy 6061-T6*, Chiang Mai Journal of Science, vol. 36, no. 3, pp. 276-286, 2009.

[30] S.H. Avner, *Introduction to physical metallurgy,* New York: McGraw-Hill, vol. 2, pp. 481-497, 1974.

[31] G. Elatharasan, V.S. Kumar, *An experimental analysis and optimization of process parameter on friction stir welding of AA 6061-T6 aluminum alloy using RSM*, Procedia Engineering, vol. 64, pp. 1227-1234, 2013, doi: 10.1016/j.proeng.2013.09.202

[32] J. Lakshmipathy, B. Kulendran, *Reciprocating wear behavior of 7075Al/SiC in comparison with 6061Al/Al_2O_3 composites*, International Journal of Refractory Metals and Hard Materials, vol. 46, pp. 137-144, 2014, doi: 10.1016/j.ijrmhm.2014.06.007

[33] M.M. Rahvard, M. Tamizifar, S.M.A. Boutorabi, S.G. Shiri, *Characterization of the graded distribution of primary particles and wear behavior in the A390 alloy ring with various Mg contents fabricated by centrifugal casting*, Materials & Design (1980-2015), vol. 56, pp. 105-114, 2014, doi: 10.1016/j.matdes.2013.10.070

[34] F. Toptan, I. Kerti, L.A. Rocha, *Reciprocal dry sliding wear behaviour of B_4Cp reinforced aluminium alloy matrix composites*, Wear, vol. 290-291, pp. 74-85, 2012, doi: 10.1016/j.wear.2012.05.007

[35] A.C. Vieira, P.D. Sequeira, J.R. Gomes, L.A. Rocha, *Dry sliding wear of Al alloy/SiCp functionally graded composites: Influence of processing conditions*, Wear, vol. 267, iss. 1-4, pp. 585-592, 2009, doi: 10.1016/j.wear.2009.01.041

[36] R.K. Uyyuru, M.K. Surappa, S. Brusethaug, *Tribological behavior of Al–Si–SiCp composites/automobile brake pad system under dry sliding conditions*, Tribology International, vol. 40, iss. 2, pp. 365-373, 2007, doi: 10.1016/j.triboint.2005.10.012

[37] A.T. Alpas, J.D. Embury, *Sliding and abrasive wear behaviour of an aluminum (2014)-SiC particle reinforced composite*, Scripta Metallurgica et Materialia, vol. 24, iss. 5, pp. 931-935, 1990, doi: 10.1016/0956-716X(90)90140-C

[38] P.L. Menezes, Kishore, S.V. Kailas, *Role of surface texture of harder surface on subsurface deformation*, Wear, vol. 266, iss. 1-2, pp. 103-109, 2009, doi: 10.1016/j.wear.2008.05.008

[39] S.C. Lim, M.F. Ashby, *Overview no. 55 wear-mechanism maps*, Acta Metallurgica, vol. 35, iss. 1, pp. 1-24, 1987, doi: 10.1016/0001-6160(87)90209-4